Exploration of the role of *EMC3-AS1* as a potential diagnostic and prognostic indicator in liver cancer

BO LIU[1,2], XIA YUAN[3], KE DONG[4], JIE ZHANG[2], TINGTING FU[5] and CHENGYOU DU[1]

[1]Department of Hepatobiliary Surgery, The First Affiliated Hospital of Chongqing Medical University, Chongqing 400016, P.R. China;

[2]Department of Hepatobiliary Surgery, Pidu District People's Hospital of Chengdu, Chengdu, Sichuan 611730, P.R. China;

[3]School of Bioscience and Technology, Chengdu Medical College, Chengdu, Sichuan 610500, P.R. China;

[4]Department of Hepatobiliary Surgery, Sichuan Provincial People's Hospital, Chengdu, Sichuan 610000, P.R. China;

[5]Department of Nosocomial Infection Control, Pidu District People's Hospital of Chengdu, Chengdu, Sichuan 611730, P.R. China

Abstract. The aim of the present study was to evaluate the diagnostic and prognostic significance of the long non-coding RNA (lncRNA) endoplasmic reticulum membrane protein complex subunit 3 antisense RNA 1 (*EMC3-AS1*) in liver cancer, and its impact on the proliferative and invasive capabilities of liver cancer cells. *EMC3-AS1* expression in liver cancer was assessed using data from The Cancer Genome Atlas and three Gene Expression Omnibus datasets, and validated in clinical liver cancer samples using reverse transcription-quantitative PCR. The prognostic and diagnostic potentials of this lncRNA were evaluated using Kaplan-Meier and receiver operating characteristic analyses, respectively. The infiltration of immune cells and differential expression of immune checkpoints (ICs) between high- and low-EMC3-AS1 expression groups were investigated. Therapeutic correlation analyses were also undertaken to assess the impact of *EMC3-AS1* in the treatment of liver cancer. In addition, *in vitro* experiments were conducted using small interfering RNA to knock down the expression of *EMC3-AS1* in HepG2, Sk-Hep-1 and Huh-7 cells, and evaluate the effect on cell proliferation, colony formation and migration. The results revealed a significant upregulation of *EMC3-AS1* expression in liver cancer tissues compared with that in adjacent normal tissues, which was associated with an unfavorable prognosis and demonstrated diagnostic effectiveness for patients with liver cancer. Furthermore, patients with high *EMC3-AS1* expression exhibited increased levels of IC markers in comparison with those with low *EMC3-AS1* expression. In addition, *EMC3-AS1* was indicated to have clinical significance in the prediction of the response to immunotherapy and chemotherapy. Notably, the *in vitro* experiments demonstrated that the knockdown of *EMC3-AS1* significantly hindered cell proliferation, colony formation and migration. Consequently, it was concluded that *EMC3-AS1* is upregulated in liver cancer and serves as a prognostic indicator for unfavorable outcomes in patients with liver cancer. Additionally, targeting *EMC3-AS1* through knockdown interventions showed potential in mitigating the ability of liver cancer cells to proliferate and migrate, which highlights its dual role as a biomarker and therapeutic target for liver cancer.

Introduction

According to 2020 Global Cancer Statistics, liver cancer accounts for 75-85% of primary liver tumors, with ~906,000 new cases diagnosed each year, and is the third most frequent cause of cancer-associated mortality worldwide (1). Due to the insidious onset of liver cancer and the absence of early clinical manifestations, the majority of patients with liver cancer are diagnosed at an advanced disease stage, which precludes surgical intervention (2). Despite advancements in treatment modalities such as liver transplantation, anatomical liver resection, interventional therapy, local ablation therapy, radiation therapy and targeted therapy, the 5-year overall survival (OS) rate remains at <15% (3).

Long non-coding RNAs (lncRNAs), a class of RNAs >200 nucleotides in length without protein translation capacity, play a pivotal role in tumorigenesis (4). Certain lncRNAs are known to be involved in various biological processes, including cell stemness, DNA damage, chemical resistance, immune escape, epithelial-mesenchymal transition (EMT) and metabolic disorders (5). The aberrant expression of lncRNA may contribute to the occurrence, progression, invasion and metastasis of diverse tumors, including liver cancer (6-9). For instance, Tang *et al* (10) identified that the expression of lncRNA *CRNDE* was upregulated in liver cancer, and promoted the proliferation and migration of liver cancer cells by sponging microRNA (miR)-337-3p, thereby upregulating the expression of sineoculis homeobox homolog 1. In another study, lncRNA *CEBPA-DT* was shown to interact with

Correspondence to: Dr Chengyou Du, Department of Hepatobiliary Surgery, The First Affiliated Hospital of Chongqing Medical University, 1 Medical College Road, Yuzhong, Chongqing 400016, P.R. China
E-mail: duchengyou@126.com

heterogeneous nuclear ribonucleoprotein C, thereby activating the interaction between discoidin domain receptor 2 and β-catenin, leading to liver cancer metastasis (11). Furthermore, lncRNA *SNHG7* was indicated to induce the proliferation and migration of liver cancer cells by sponging miR-122-5p (12), and lncRNA *ANRIL* was demonstrated to regulate liver cancer cell proliferation, migration and invasion via the targeting of miR-384 and modulation of STAT3 (13).

The formation of N6-methyladenosine (m6A) is a frequently occurring epigenetic modification that is essential for mRNA splicing, export, translation and degradation, and has been shown to play an important role in the occurrence and progression of numerous malignancies (14). Previous studies have demonstrated that lncRNAs regulate m6A modifications in various types of cancer (15). Endoplasmic reticulum membrane protein complex subunit 3 antisense RNA 1 (*EMC3-AS1*) is an lncRNA located on chromosome 3q25. A correlation analysis performed in our preliminary screening analysis (unpublished data) revealed that the expression of *EMC3-AS1* positively correlates with that of m6A-associated genes in liver cancer, including methyltransferase-like 3, RNA-binding motif protein 15B, YTH N6-methyladenosine RNA-binding protein F1, heterogeneous nuclear ribonucleoprotein A2/B1 and RNA-binding motif protein X-linked. However, the expression and function of lncRNA *EMC3-AS1* have not yet been thoroughly explored in liver cancer.

In the current study, the differential expression of *EMC3-AS1* between liver cancer tissues and adjacent normal (AN) liver tissues was identified by the analysis of data from The Cancer Genome Atlas (TCGA) and three Gene Expression Omnibus (GEO) datasets, and subsequently validated in a primary clinical cohort. The potential association of *EMC3-AS1* expression with the prognosis and diagnosis of patients with liver cancer was then explored. The tumor microenvironment (TME) was also compared between liver cancer tissues with high (H) and low (L) expression of *EMC3-AS1*. Additionally, *EMC3-AS1* was silenced using small interfering RNA (siRNA) in HepG2, Sk-Hep-1 and Huh-7 liver cancer cells, and cell proliferation, colony formation and migration were evaluated *in vitro*.

Materials and methods

Data acquisition and expression analysis. Gene expression data, comprising fragments per kilobase of transcripts per million mapped reads, and the respective clinical data of patients with liver cancer were obtained from TCGA (http://cancergenome.nih.gov/). Subsequently, the format of the gene expression data was converted into transcripts per million reads values for analysis. In addition, three datasets (GSE22058, GSE25097 and GSE64041) (16-18) containing data on 428 tumor specimens and 451 AN specimens were downloaded from the GEO database (https://www.ncbi.nlm.nih.gov/geo/) for the validation of *EMC3-AS1* expression (Table SI). The expression of *EMC3-AS1* was compared between tumor and AN tissues in the datasets from TCGA and the GEO, and 50 pairs of liver cancer tissues and AN tissues from the same patients in TCGA were compared as well.

Collection of patients and tissue specimens. A total of 42 liver cancer and 35 AN tissues (at least 2 cm away from the tumor edge) were acquired from patients with liver cancer (n=42; mean age, 60.1 years*;* age range, 35-80 years) who underwent liver resection in Sichuan Provincial People's Hospital (Chengdu, China) between January 2022 and September 2022. Information on each patient is listed in Table SII. Patients in this study were diagnosed with liver cancer by preoperative imaging examination or biopsy, and their preoperative liver function was classified as Child-Pugh grade A (19). None of the patients underwent preoperative therapy. Patients with cholangiocarcinoma or metastatic liver cancer were excluded. After resection, all tissue specimens were promptly frozen in liquid nitrogen and preserved at -80°C. The present study was conducted in compliance with the Declaration of Helsinki and was approved by the Ethics Committee of Sichuan Provincial People's Hospital (approval no. 2022-2). Before surgery, all patients provided written informed consent for the use of their tissue samples in the present study.

RNA extraction and reverse transcription-quantitative PCR (RT-qPCR). Total RNA was isolated from liver cancer and normal liver tissues using TRIzol® (Invitrogen; Thermo Fisher Scientific, Inc.). A NanoDrop spectrophotometer (NanoDrop Technologies; Thermo Fisher Scientific, Inc.) was utilized to examine the yield and purity of the RNA samples. A 260/280 optical density ratio of 1.8-2.2 was considered to indicate acceptable RNA purity. Agarose gel electrophoresis was then conducted, and the integrity and diffusion of the bands were examined to assess the quality of the total RNA. Samples displaying RNA degradation during collection were excluded to ensure the accuracy and reliability of the experimental data. Subsequently, cDNA synthesis was conducted using a PrimeScript™ RT Reagent kit with DNA Eraser (Takara Bio, Inc.) according to the manufacturer's instructions. qPCR was then conducted using TB-Green®-Premix-Ex-Taq™-II (Takara Bio, Inc.). *EMC3-AS1* and *GAPDH* gene products were amplified, with the latter serving as the reference gene. qPCR was performed under the following conditions: 95°C for 30 sec, then 40 cycles of 95°C for 5 sec, 55°C for 30 sec and 72°C for 1 min, followed by 95°C for 10 sec and 65°C for 5 sec. The primers used were as follows: *GAPDH* forward, 5'-ACA TCGCTCAGACACCATG-3' and reverse, 5'-ACCAGAGTT AAAAGCAGCCC-3'; and *EMC3-AS1* forward, 5'-TGC CTCAGTATCTGAACACAAG-3' and reverse, 5'-TTGAGC CAGGGACATTTCTG-3'. Relative expression level was obtained using the $2^{-\Delta\Delta Cq}$ method (20).

Prognostic and diagnostic value of EMC3-AS1. Patients with liver cancer from TCGA were categorized into H-EMC3-AS1 and L-EMC3-AS1 expression groups according to the median *EMC3-AS1* expression value. Kaplan-Meier analysis and the log-rank test were used to compare OS and disease-free survival (DFS) between the H- and L-EMC3-AS1 expression groups using the survival (version 3.3) package in the R platform. The pROC (version 1.18) (21) package was used to perform receiver operating characteristic (ROC) curve analysis on the aforementioned datasets and the present cohort.

Functional enrichment analysis. Gene set variation analysis (GSVA) was performed to assess the variation of pathways between the H- and L-EMC3-AS1 expression groups using the GSVA (version 1.44.2) package in R (22), and the data were displayed using heatmaps. Hallmark and Kyoto Encyclopedia of Genes and Genomes (KEGG) gene sets were acquired from MSigDB (23). Gene set enrichment analysis (GSEA) was carried out to determine the differential functional phenotype between the H- and L-EMC-AS1 expression groups using the clusterProfiler (version 4.4.4) (24) package. A false discovery rate (FDR) of <0.05 was used as the cut-off threshold for significantly enriched gene sets. The limma (version 3.52.1) (25) package was employed to identify differentially expressed mRNAs (DEmRNAs) between the H- and L-EMC-AS1 expression groups. Genes with a |log2 fold-change (FC)|>1 and FDR <0.05 were selected as DEmRNAs. Gene Ontology (GO) and KEGG pathway analyses were performed using the clusterProfiler package. Adjusted P<0.05 was used as the cut-off threshold for GO terms and KEGG pathways.

Analysis of EMC3-AS1 as a risk factor for OS and its association with clinicopathological features. Univariate and multivariate Cox regression analyses were conducted to screen for the risk factors for poor prognosis (shorter OS time) in patients with liver cancer. Subgroup analyses for *EMC3-AS1* expression were conducted based on age, sex, tumor stage, pathological stage, tumor grade, Child-Pugh stage, bilirubin level, α-fetoprotein (AFP) level and vascular invasion status. The 7th American Joint Committee on Cancer staging system was used for staging (26).

Association of EMC3-AS1 expression with tumor-infiltrating immune cells (TIICs). CIBERSORT (version 1.06) (27) is a deconvolution algorithm used to distinguish 22 human immune cell subtypes based on the gene expression in complex tissues. The CIBERSORT algorithm was used to determine the fraction of TIICs in the tumor environment, and the associations between the infiltration of 22 subtypes of immune cells and EMC3-AS1 expression in liver cancer were determined.

Immune checkpoint (IC) inhibitors (ICIs) have markedly changed cancer treatment in recent decades (28). Thus, the mRNA expression levels of 35 ICs, such as cytotoxic T-lymphocyte antigen 4 (*CTLA4*), programmed cell death protein 1 (*PDCD1*), *CD86*, *CD274*, *CD276*, hepatitis A virus cellular receptor 2 (*HAVCR2*), lymphocyte-activation gene 3 (*LAG3*), galectin 9 (*LGALS9*), neuropilin 1 (*NRP1*) and T cell immunoreceptor with Ig and ITIM domains (*TIGIT*), among others, were compared between the H- and L-EMC-AS1 expression groups in the present study.

The activity of cancer stem cells (CSCs) can be quantified using the mRNA stemness index (mRNAsi) and epigenetically regulated mRNAsi (EREG-mRNAsi) (29), which reflect the dedifferentiation capacity of CSCs. Therefore, the score of mRNAsi and EREG-mRNAsi obtained from previous research (29) were compared between the H- and L-EMC3-AS1 expression groups. Pearson's correlation analysis was applied to investigate the correlations between the expression of EMC3-AS1 and mRNAsi or EREG-mRNAsi. Furthermore, ESTIMATE score, immune score and stromal score generated by ESTIMATE algorithm (30) could reflect tumor immune infiltration level. These scores of patients with liver cancer in TCGA were obtained from the ESTIMATE database (https://bioinformatics.mdanderson.org/estimate/) and were compared between H- and L-EMC3-AS1 expression groups, respectively. Additionally, the activities of 13 immune-associated pathways were evaluated using the single-sample GSEA (ssGSEA) algorithm in GSVA (version 1.44.2) package (21), and comparisons between the H- and L-EMC3-AS1 expression groups were made.

Therapeutic correlation analyses. The immunophenoscore (IPS) is a scoring scheme ranging from 0 to 10 that reflects the response of patients with cancer to anti-CTLA4 and anti-programmed cell death protein 1 (PD-1) therapy (31). IPSs were obtained from The Cancer Immunome Atlas (TCIA; https://tcia.at/home), and were compared between the H- and L-EMC3-AS1 expression groups to assess the association between immunotherapy response and *EMC3-AS1* expression in liver cancer.

The tumor immune dysfunction and exclusion (TIDE) scoring scheme (32) is a predictor of the response to IC blockade in patients with cancer. The TIDE score of patients with liver cancer was computed using the TIDE online tool (http://tide.dfci.harvard.edu), and the TIDE scores of the H- and L-EMC3-AS1 expression groups were compared. Furthermore, the oncoPredict (version 0.2) package (33) was used to compute the half-maximal inhibitory concentrations of various chemotherapeutic and molecular targeted drugs for the treatment of liver cancer, and the difference in drug sensitivity between the H- and L-EMC3-AS1 expression groups was then compared.

Cell culture, transfection and treatment. HepG2, Sk-Hep-1 and Huh-7 cells were obtained from The Cell Bank of Type Culture Collection of The Chinese Academy of Sciences and were authenticated using STR profiling. The HepG2 and Huh-7 cell lines were cultured in high-glucose DMEM (Gibco; Thermo Fisher Scientific, Inc.) containing 10% FBS (Biological Industries; Sartorius AG) and 1% streptomycin-penicillin (Biological Industries; Sartorius AG), while the Sk-Hep-1 cells were cultured in minimum essential medium (Gibco; Thermo Fisher Scientific, Inc.) containing 10% FBS and 1% streptomycin-penicillin. Cells were maintained in a 37°C incubator with 5% CO_2.

The HepG2, Sk-Hep-1 and Huh-7 cells were transfected with siRNAs (Shanghai GenePharma Co., Ltd.) using Lipofectamine® 2000 (Invitrogen; Thermo Fisher Scientific, Inc.) at a final concentration of 200 nM. After 48 h of transfection at 37°C, total RNA was extracted. The efficacy of the siRNA transfection was assessed to determine the interference efficiency. The siRNAs demonstrating the highest interference efficacy were chosen for further analyses. The siRNA sequences were as follows: EMC3-AS1-negative control (NC) sense, 5'-UUCUCCGAACGUGUCACGUTT-3' and antisense, 5'-ACGUGACACGUUCGGAGAATT-3'; EMC3-AS1-1739 sense, 5'-GUGCCACCAUGGAUAUUCATT-3' and antisense, 5'-UGAAUAUCCAUGGUGGCACTT-3'; EMC3-AS1-2842 sense, 5'-CCACCAGAUAUACCACUAUTT-3' and antisense, 5'-AUAGUGGUAUAUCUGGUGGTT-3'.

Colony formation assay. Following transfection, the HepG2, Sk-Hep-1 and Huh-7 cells (2,000 cells/well) were independently cultured in 6-well plates and incubated for 14 days. Subsequently, the cells were fixed with 4% paraformaldehyde for 20 min at room temperature and stained with crystal violet (0.5%; Sigma-Aldrich; Merck KGaA) for 15-20 min at room temperature. A cluster with >50 cells was defined as a colony. Colony numbers were calculated using ImageJ software (Version 1.52; National Institutes of Health), and representative images were captured.

Cell proliferation assay. To detect cell proliferation, MTT (Sigma-Aldrich; Merck KGaA) was added to transfected HepG2, Sk-Hep-1 and Huh-7 cells. The cells (4,000 cells/well) were seeded in a 96-well plate (100 μl/well) and cultured. After 24, 48, 72 or 96 h of transfection, 100 μl MTT was added and the cells were incubated for another 4 h. Next, the supernatant was removed, and DMSO was added (150 μl/well). The absorbance at 490 nm was recorded using a microplate reader after shaking on an orbital shaker for 10 min.

Wound healing assay. Transfected cells were plated in a 6-well culture plate after transfection. Upon reaching >90% cell confluence, the wound was gently scraped with a 100-μl pipette tip and a sterile ruler. After scraping, the cells were rinsed three times with PBS to eliminate the detached cells, and 2 ml DMEM containing 2% FBS was added to each well followed by incubation. Images were captured and the migration distance was measured by comparing the images at 0 h and after culturing the cells for 24 h. An inverted microscope (Olympus Corporation) was used to calculate the number of migrated cells.

Transwell assay. Cell suspensions containing $5x10^4$ cells were added to the upper chamber of a 24-well culture plate with Transwell inserts and incubated with serum-free DMEM (200 μl) at 24 h post-transfection. In the lower chamber of the 24-well plates, 500 μl complete DMEM was added. Following 24 h of incubation at 37˚C, the chambers were removed and rinsed once with sterile PBS. Cells on the upper side were wiped away with a cotton swab. The remaining cells were fixed for 15 min and stained with crystal violet (0.5%) for 20 min at room temperature. Finally, a light microscope was employed to collect images and count the number of migrated cells.

Statistical analysis. Statistical analysis and plotting were performed in R software (version 4.0) and GraphPad Prism (version 8.0; Dotmatics). Univariate and multivariate Cox regression analyses were used to identify prognostic factors associated with OS. Survival curves were generated and compared between different EMC3-AS1 expression groups using Kaplan-Meier analysis and the log-rank test. For continuous variables with non-normal distributions, Wilcoxon rank-sum test was applied for comparing differences between two independent groups, while Wilcoxon signed-rank test was used for paired groups. All experiments were performed in triplicate. Data from the experiments are expressed as the mean ± standard deviation. Differences among multiple groups

were compared by one-way analysis of variance followed by Dunnett's post hoc test. P<0.05 was considered to indicate a statistically significant result.

Results

EMC3-AS1 is upregulated in liver cancer tissues. Analysis of data from TCGA revealed a significant upregulation of *EMC3-AS1* in 374 liver cancer tissues compared with that in 50 AN tissues, as well as in 50 paired liver cancer samples compared with AN tissues (P<0.001; Fig. 1A and B). *EMC3-AS1* upregulation was also evident in the tumor tissues in the three GEO datasets containing 428 liver cancer and 451 AN tissues (P<0.001; Fig. 1C-E). In addition, based on the results of RT-qPCR analysis of the current study cohort, *EMC3-AS1* expression was upregulated in the 42 liver cancer tissues compared with that in the 35 AN liver tissues (P<0.001; Fig. 1F).

EMC3-AS1 is both an unfavorable prognostic biomarker and an effective diagnostic biomarker. Kaplan-Meier analysis revealed that the patients in the H-EMC3-AS1 group exhibited shorter OS (P=0.005) and DFS times (P<0.001) compared with those in the L-EMC3-AS1 group (Fig. 2A and B). In the ROC analysis based on *EMC3-AS1* expression in HCC and adjacent tissues, the area under the curve (AUC) in TCGA cohort was 0.866 (Fig. 2C). The good performance of *EMC3-AS1* was validated in the GEO datasets GSE22058, GSE25097 and GSE64041, with AUCs of 0.892, 0.824 and 0.703, respectively (Fig. 2D-F). In addition, ROC analysis was conducted to examine the ability of *EMC3-AS1* expression to distinguish liver cancer in the current study cohort. Notably, it was found that *EMC3-AS1* exhibited good diagnostic ability, with an AUC of 0.785 (Fig. 2G).

EMC3-AS1 is a significant prognostic factor. The univariate Cox regression analysis (Fig. 3A) indicated that poor prognosis was associated with the expression of *EMC3-AS1* [hazard ratio (HR), 1.32; 95% confidence interval (CI), 1.15-1.53; P<0.001], tumor stage (HR, 2.59; 95% CI, 1.82-3.69; P<0.001) and pathological stage (HR, 2.49; 95% CI, 1.71-3.61; P<0.001). In the multivariate Cox regression analysis (Fig. 3A), shorter OS time was found to be independently associated with the expression of *EMC3-AS1* (HR, 1.24; 95% CI, 1.07-1.45; P=0.006) and advanced tumor stage (HR, 2.30; 95% CI, 1.58-3.37; P<0.001). In the subgroup analysis, patients with liver cancer who had an advanced tumor stage (P=0.005), advanced pathological stage (P=0.005), advanced histological grade (P<0.001) and higher AFP level (P=0.004) were found to have significantly elevated *EMC3-AS1* expression levels (Fig. 3B). However, no notable differences in *EMC3-AS1* expression were observed between the subgroups based on age, sex, Child-Pugh stage, bilirubin level or vascular invasion status.

Functional enrichment analysis. According to the result of GSVA, the Hallmark gene sets 'G$_2$M checkpoint', 'E2F targets' and 'mitotic spindle' were markedly activated in the H-*EMC3-AS1* expression group (Fig. 4A). In the KEGG gene sets, pathways associated with cell division and proliferation, including 'DNA replication' and 'cell cycle', were markedly
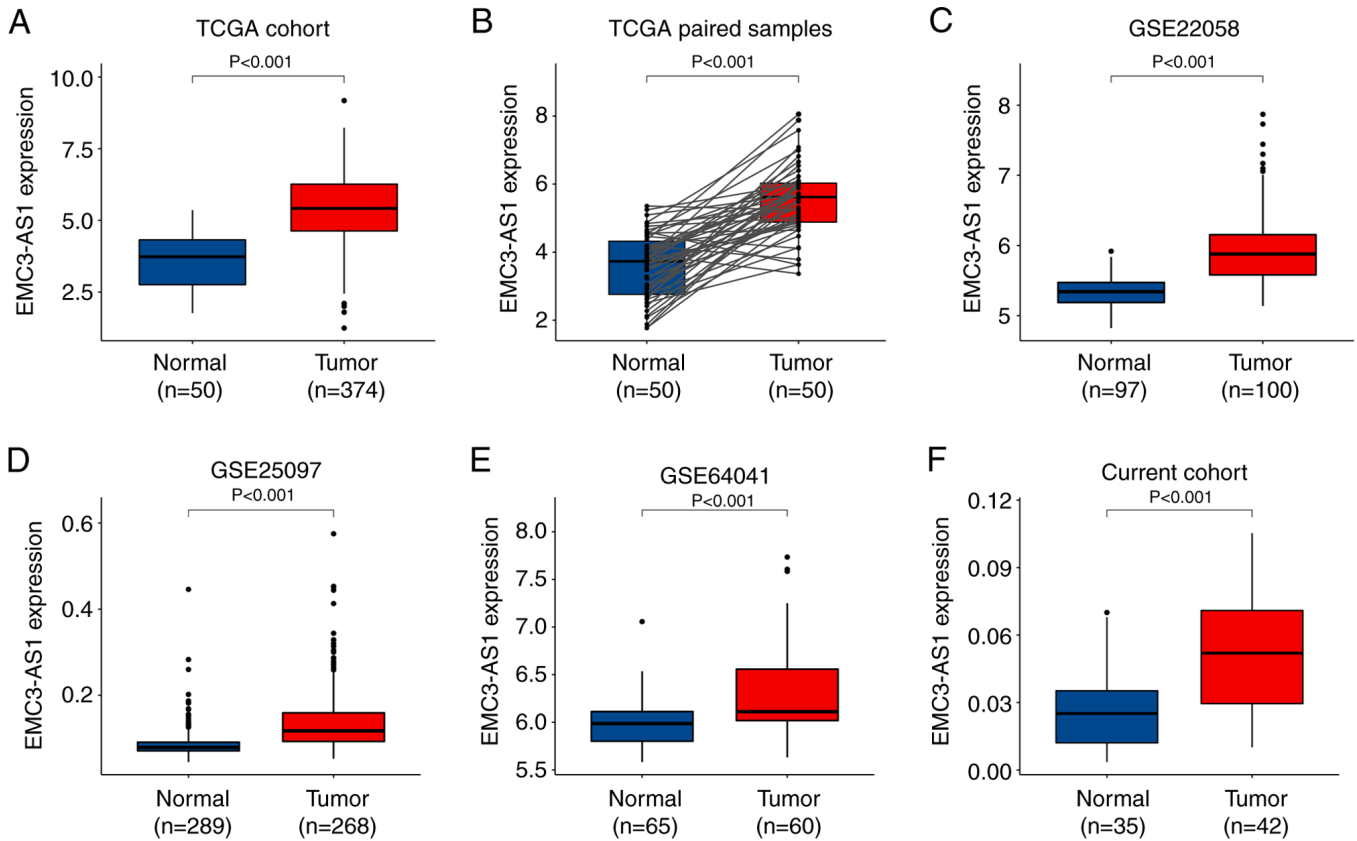
Figure 1. Expression of *EMC3-AS1* in liver cancer. The expression of *EMC3-AS1* was compared between (A) liver cancer and AN tissues in TCGA, (B) paired liver cancer tissues and AN tissues in TCGA, and (C-E) liver cancer tissues and AN tissues in three Gene Expression Omnibus datasets. (F) *EMC3-AS1* expression in liver cancer measured using reverse transcription-quantitative PCR in a primary clinical cohort. EMC3-AS1, endoplasmic reticulum membrane protein complex subunit 3 antisense RNA 1; AN, adjacent normal; TCGA, The Cancer Genome Atlas.

enriched in the H-EMC3-AS1 expression group (Fig. 4B). A total of 222 DEmRNA (180 upregulated and 42 downregulated genes) were identified between the H- and L-EMC3-AS1 expression groups. For these DEGs, GO enrichment analysis revealed that 'nuclear division', 'chromosomal region' and 'tubulin binding' were the most enriched terms in the biological process, cellular component and molecular function categories (Fig. 4C; Table SIII). 'Progesterone-mediated oocyte maturation', 'cell cycle' and 'oocyte meiosis' were found to be the most highly enriched pathways in the KEGG pathway enrichment analysis (Fig. 4E; Table SIV).

In the GSEA, 'E2F targets', 'G$_2$M checkpoint' and 'mitotic spindle' were the top three enriched pathways in the Hallmark gene sets, while 'intrinsic pathway of fibrin clot formation', 'cytochrome p450 arranged by substrate type' and 'formation of fibrin clot clotting cascade' were the most enriched Reactome gene sets (Fig. 4D and F).

Association of EMC3-AS1 expression with immune status. The expression of *EMC3-AS1* was found to be positively correlated with the infiltration of activated memory CD4 T cells (R=0.17, P=0.001), follicular helper T cells (R=0.15, P=0.004), regulatory T cells (R=0.15, P=0.003), M0 macrophages (R=0.18, P<0.001) and neutrophils (R=0.15, P=0.004), and negatively correlated with the infiltration of resting memory CD4 T cells (R=-0.12, P=0.026) and monocytes (R=-0.14, P=0.007)

(Fig. 5A). The mRNA levels of the ICs *CTLA4*, *PDCD1*, *CD86*, *CD274*, *CD276*, *HAVCR2*, *LAG3*, *LGALS9*, *NRP1* and *TIGIT* were significantly higher in the H-EMC3-AS1 expression group compared with those in the L-EMC3-AS1 expression group (P<0.05*;* Fig. 5B). In addition, the mRNAsi of the H-EMC3-AS1 group was higher than that of the L-EMC3-AS1 group (P=0.004; Fig. 5C) and was positively correlated with *EMC3-AS1* expression (R=0.17, P=0.001). By contrast, the EREG-mRNAsi of the H-EMC3-AS1 group was lower than that of the L-EMC3-AS1 group (P=0.001), and was negatively correlated with *EMC3-AS1* expression (R=-0.21, P<0.001; Fig. 5D). Additionally, the Stromal score (P=0.003) and Estimate score (P=0.023) of patients in the H-EMC3-AS1 group were significantly lower than those of patients in the L-EMC3-AS1 group (Fig. 5E). According to the result of the ssGSEA for 13 immune-related pathways, the activity of MHC class I molecules was greater in the H-EMC3-AS1 group compared with that in the L-EMC3-AS1 group (P<0.001), whereas type I/II IFN responses and cytolytic activity were restrained in the H-EMC3-AS1 expression group (P<0.001, Fig. 5F).

Comprehensive therapeutic analysis. IPS analysis indicated that the IPS level of patients in the L-EMC3-AS1 group was elevated compared with that of the H-EMC3-AS1 group, suggesting that patients in the L-EMC3-AS1 expression
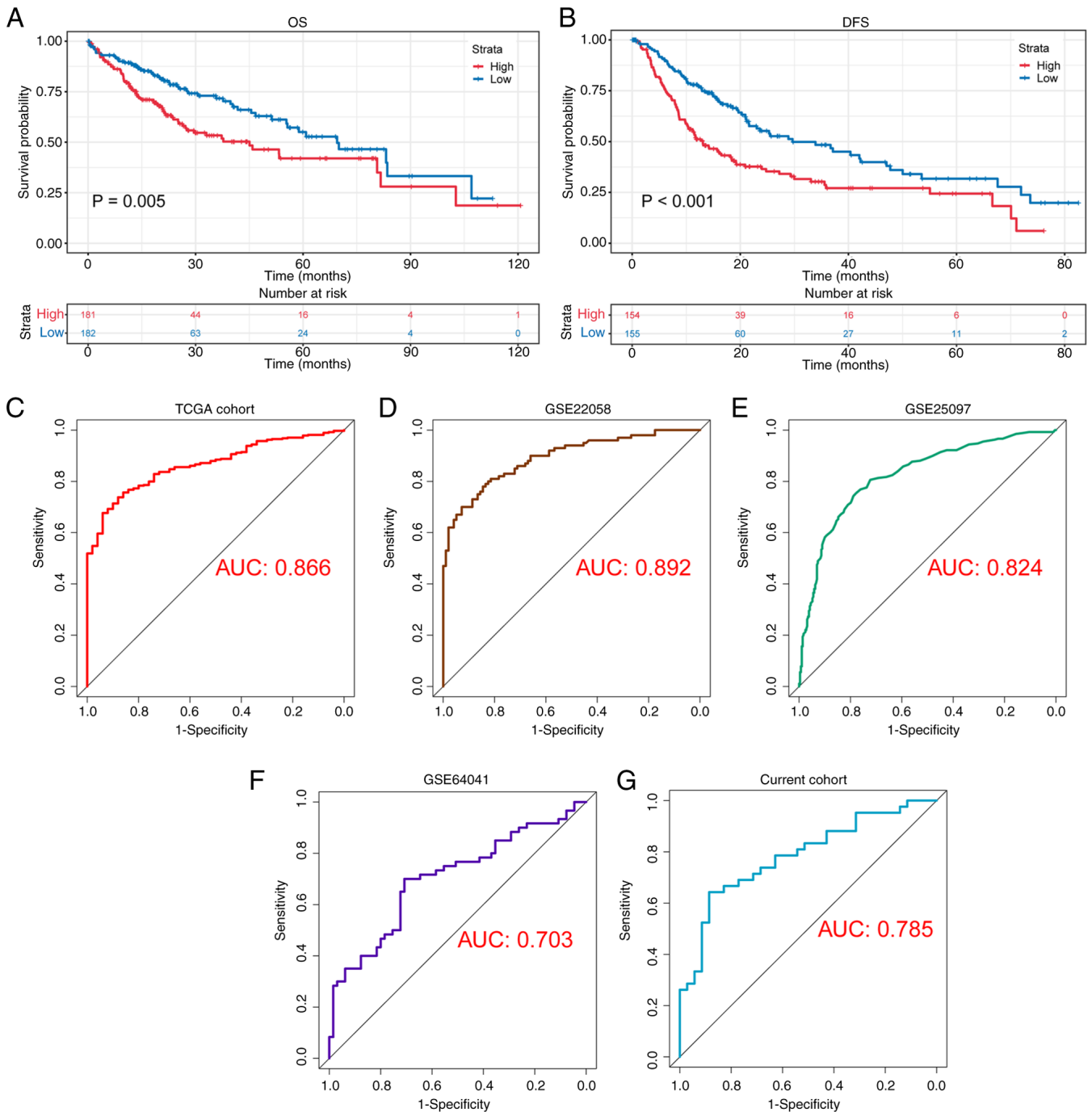
Figure 2. Prognostic and diagnostic value of *EMC3-AS1* in liver cancer. Higher expression of *EMC3-AS1* was significantly associated with (A) poorer OS and (B) poorer DFS in liver cancer. (C) Receiver operating characteristic curve for *EMC3-AS1* expression in liver cancer and adjacent tissues from TCGA. (D-F) Validation of the diagnostic value of *EMC3-AS1* in three datasets from the Gene Expression Omnibus and (G) the current clinical cohort. EMC3-AS1, endoplasmic reticulum membrane protein complex subunit 3 antisense RNA 1; OS, overall survival; DFS, disease-free survival; TCGA, The Cancer Genome Atlas; AUC, area under the curve.

group were more suitable for immunotherapy (P=0.013). Furthermore, patients in L-EMC3-AS1 expression group also demonstrated significantly higher IPS-CTLA4 blocker scores (P=0.015) and IPS-CTLA4-PD1 blocker scores (P=0.047), which suggested that these patients might experience an effective response when treated with anti-CTLA4 or anti-PD1 plus anti-CTLA4 therapy (Fig. 6A). In the TIDE analysis, lower dysfunction scores and higher exclusion scores of T cells in the tumor microenvironment were found in patients with high *EMC3-AS1* expression compared with those in patients

with low *EMC3-AS1* expression (P=0.001 and P=0.002, respectively; Fig. 6B). Furthermore, the oncoPredict analysis indicated that the patients in the L-EMC3-AS1 group would be more sensitive to treatment with entinostat, erlotinib, oxaliplatin, palbociclib and selumetinib compared with those in the H-EMC3-AS1 group (all P<0.05; Fig. 6C).

Silencing EMC3-AS1 inhibits liver cancer cell proliferation. HepG2, Sk-Hep-1 and Huh-7 cells were transfected with non-targeting siRNA (siRNA-NC) or EMC3-AS1-specific
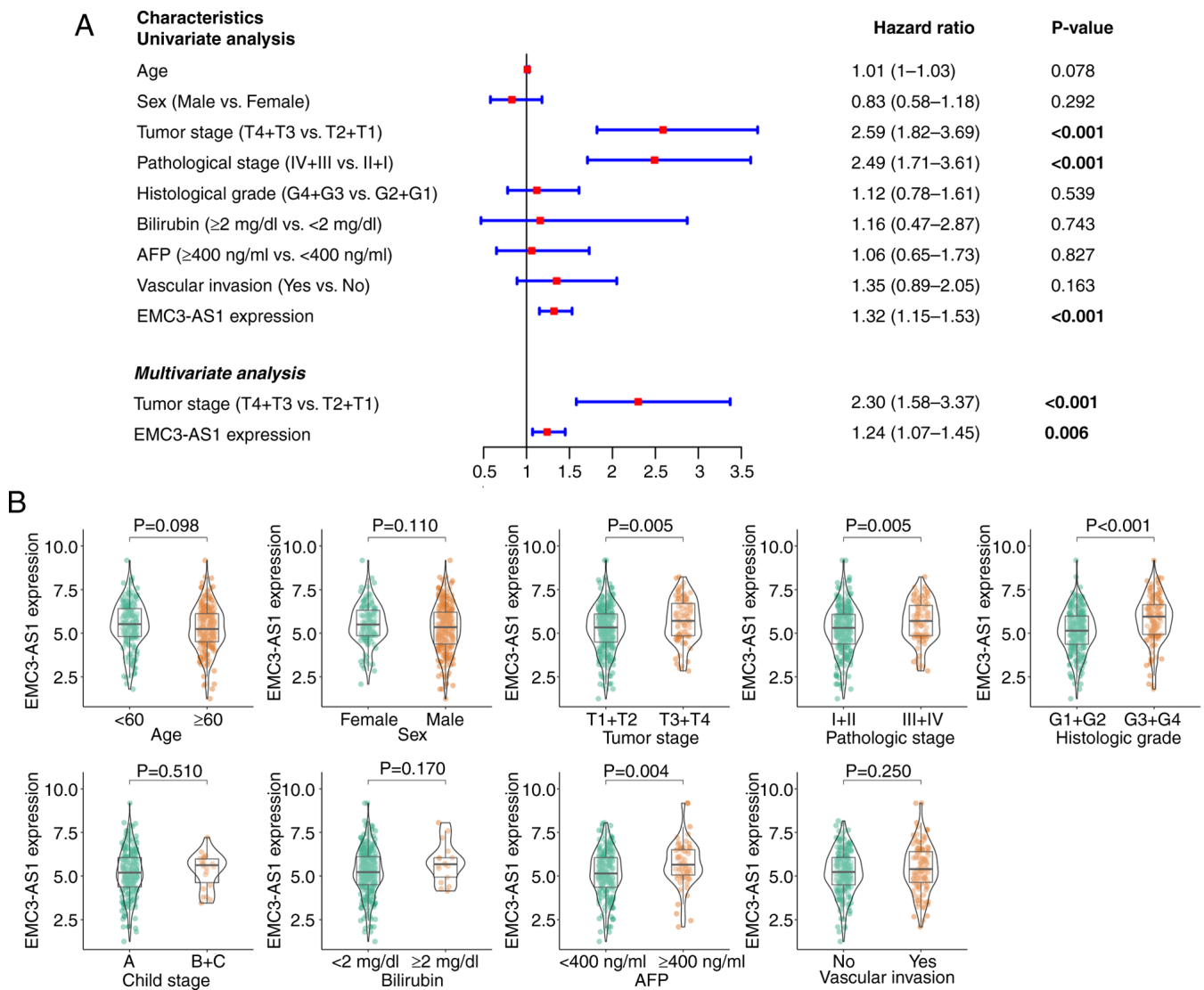
Figure 3. Analysis of the clinical value of *EMC3-AS1* in liver cancer. (A) Univariate and multivariate Cox regression analysis of *EMC3-AS1* for the overall survival of liver cancer based on data in The Cancer Genome Atlas. (B) Differential of expression of *EMC3-AS1* in subgroups based on clinicopathological characteristics. In the violin plots, the green and orange dots represent the expression of *EMC3-AS1* in samples from different clinical groups. EMC3-AS1, endoplasmic reticulum membrane protein complex subunit 3 antisense RNA 1; AFP, α-fetoprotein.

siRNAs (siRNA-1739/2842) to silence the expression of *EMC3-AS1*. According to the results of RT-qPCR, *EMC3-AS1* expression was successfully knocked down via transfection with siRNA-1739 and siRNA-2842 in the HepG2, Sk-Hep-1 and Huh-7 cells (Fig. 7A-C), indicating that the siRNA-silenced cells were suitable for use in subsequent assays. Transfection with siRNA-1739 and siRNA-2842 was shown to reduce the proliferation and colony forming ability of HepG2, Sk-Hep-1 and Huh-7 cells compared with that of the siRNA-NC group (Fig. 7D-L).

Silencing EMC3-AS1 suppresses liver cancer cell migration. As shown in Fig. 8, the migration ability of the HepG2, Sk-Hep-1 and Huh-7 liver cancer cells in the wound healing assay was significantly reduced by the knockdown of *EMC3-AS1* expression (Fig. 8). The migration of HepG2, Sk-Hep-1 and Huh-7 cells in the Transwell assay was also significantly inhibited after the knockdown of EMC3-AS1 (Fig. 9). These results suggest that a deficiency in EMC3-AS1 affects the vital functions of liver cancer cells, and that EMC3-AS1 may serve as a novel target for liver cancer treatment.

Discussion

The current study demonstrated that the expression of *EMC3-AS1* was upregulated in liver cancer tissues compared with that in AN tissues in various datasets, including TCGA and GEO datasets, as well as in a primary clinical cohort. The expression of *EMC3-AS1* was also higher in patients with more advanced liver cancer. Higher expression of *EMC3-AS1* was associated with shorter OS and DFS times in patients with liver cancer. Furthermore, *EMC3-AS1* demonstrated the ability to effectively discriminate between liver cancer and normal tissues, exhibiting a good performance not only in TCGA and GEO datasets, but also in the current clinical cohort. These findings suggest that *EMC3-AS1* holds potential as a diagnostic and prognostic biomarker. Multivariate Cox regression analysis indicated that higher expression of *EMC3-AS1* was
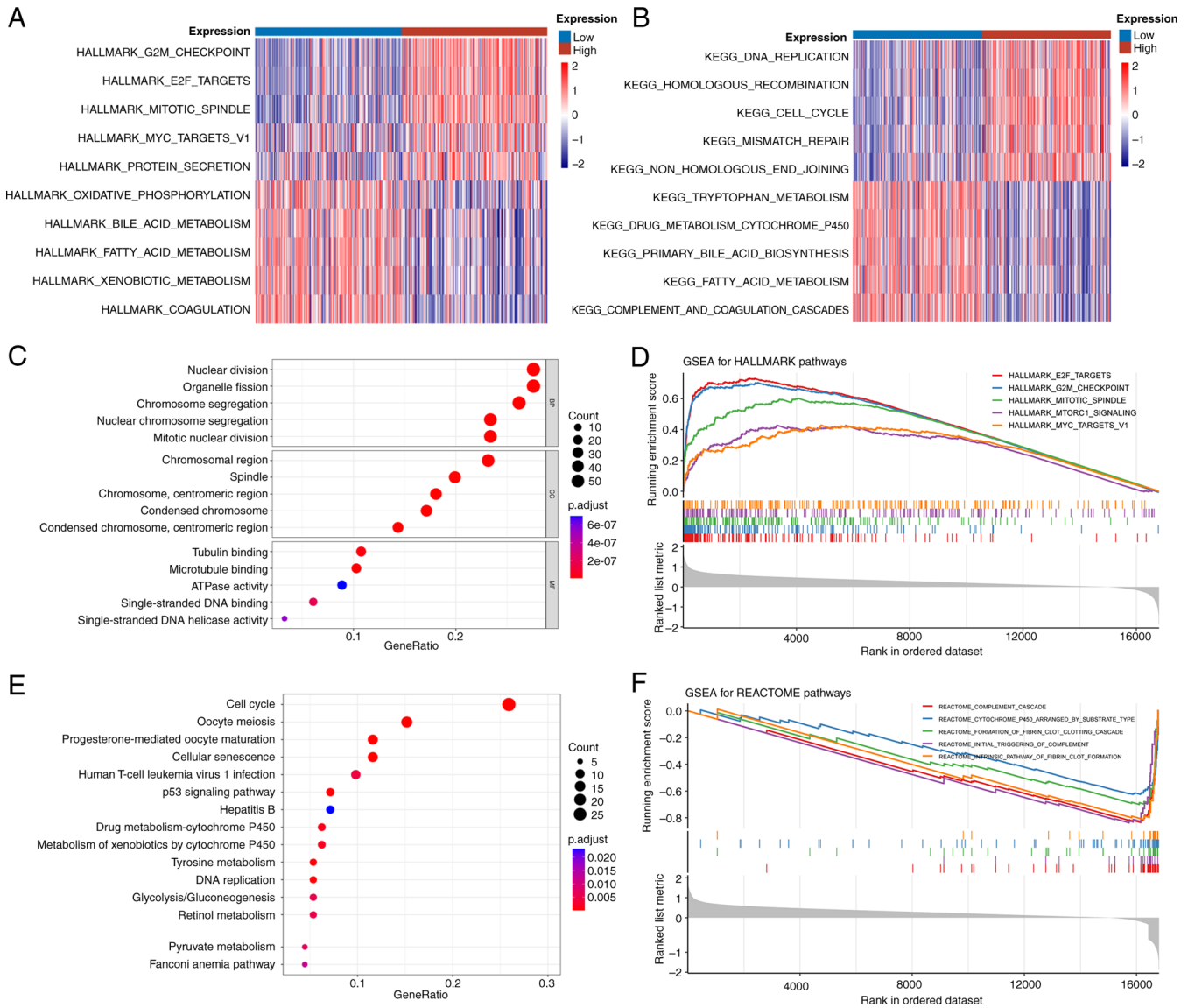
Figure 4. Functional enrichment analysis of *EMC3-AS1* in liver cancer. Heatmaps displaying the variation of (A) Hallmark and (B) KEGG pathways between high- and low-EMC3-AS1 expression groups using gene set variation analysis. (C) Dot plot of enriched Gene Ontology terms. (D) The top 5 significantly enriched pathways determined using the gene set enrichment analysis of Hallmark gene sets. (E) Dot plot of enriched KEGG pathways. (F) The top 5 significantly enriched pathways determined by the GSEA of Reactome gene sets. EMC3-AS1, endoplasmic reticulum membrane protein complex subunit 3 antisense RNA 1; KEGG, Kyoto Encyclopedia of Genes and Genomes; GSEA, gene set enrichment analysis.

independently associated with a poor prognosis in patients with liver cancer. Furthermore, GSVA, GSEA, GO and KEGG enrichment analyses showed significant enrichment and activation of several pathways associated with the tumorigenesis and progression of liver cancer, including 'chromosome segregation', 'organelle fission', 'nuclear division' and 'cell cycle'.

The TME is primarily composed of immune cells, extracellular matrix, cytokines and cancer cells (34). In addition to playing a crucial role in tumor recognition and clearance, the TME also contributes to immune escape and cancer progression (35). The TME of liver cancer is strongly suppressive, with aberrant accumulation of immunosuppressive cells (36). Immunotherapy targeting immunosuppressive cells and pathways is a promising approach for cancer treatment (37). Tumor-associated neutrophils have been identified as key drivers of progression and immunosuppression in liver cancer (38,39). Wang *et al* (40) suggested that the resistance

of hepatocellular carcinoma cells to sorafenib could be ascribed to the activation of CXCR2 signaling facilitated by tumor-associated macrophages. Regulatory T cells have also been shown to be associated with liver cancer invasion and to be crucial in hindering the development of effective antitumor responses (41). In the present study, *EMC3-AS1* expression was shown to be positively correlated with the infiltration of follicular helper T cells, activated memory CD4 T cells, M0 macrophages, regulatory T cells and neutrophils in the liver. Conversely, a significant negative correlation was observed between *EMC3-AS1* expression and the infiltration of monocytes and resting memory CD4 T cells.

ICIs have demonstrated marked therapeutic efficacy for a variety of cancer types, including liver cancer (42-44). Assessing the expression of ICs and their ligands in the TME is often the initial step when making decisions regarding immunotherapy in patients with cancer (45). In liver cancer,
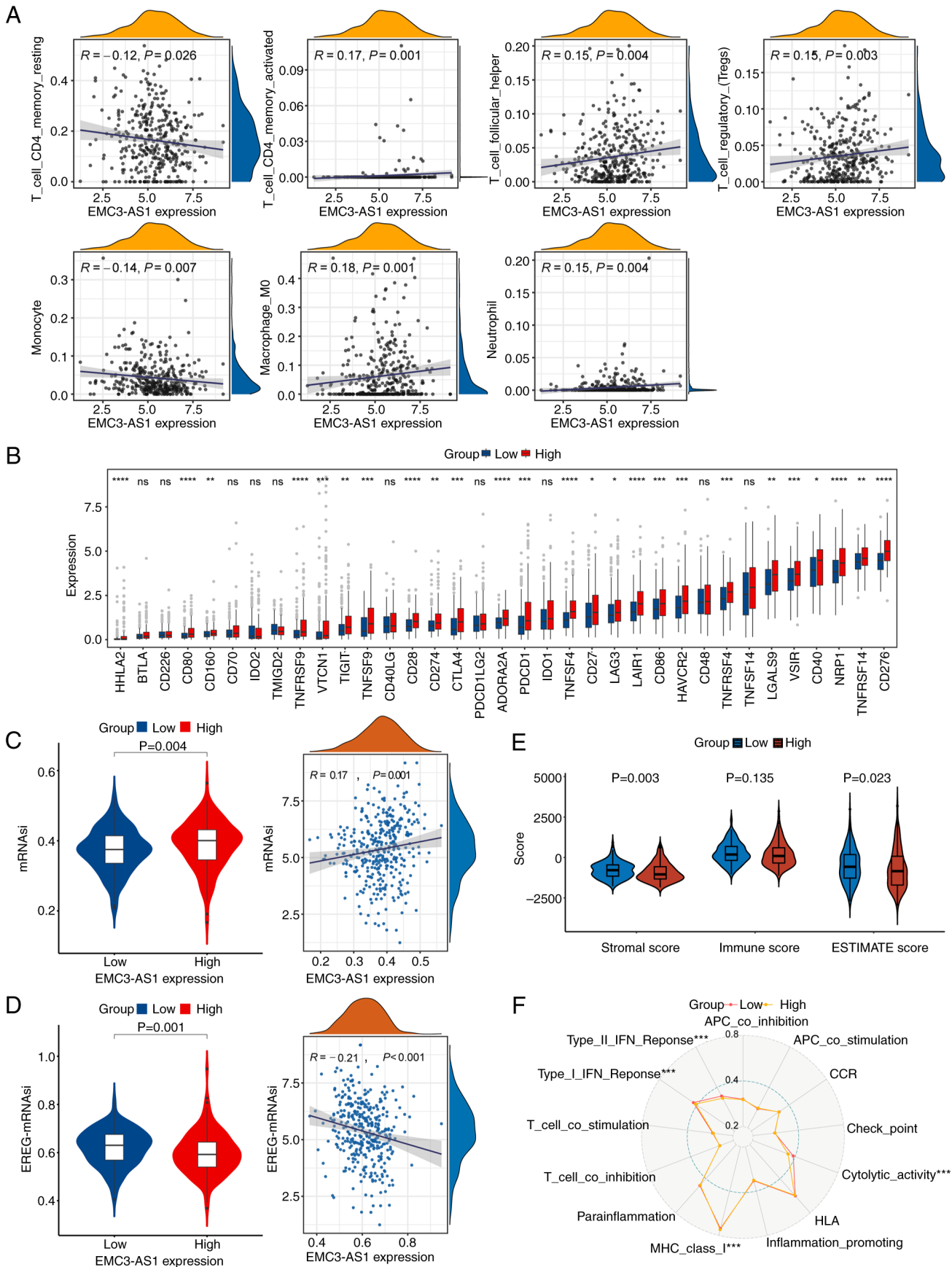
Figure 5. Immune analysis of *EMC3-AS1* in liver cancer. (A) Correlations between the expression of *EMC3-AS1* and the number of infiltrating immune cells of different types. (B) Comparison of the expression of common immune checkpoints between H- and L-EMC3-AS1 expression groups. Correlations between the expression of *EMC3-AS1* and (C) mRNAsi and (D) EREG-mDNAsi. (E) Comparison of stromal, immune and estimate scores between H- and L-EMC3-AS1 groups. (F) Comparison of the activity of 13 immune-related pathways between H- and L-EMC3-AS1 expression groups. *P<0.05, **P<0.01, ***P<0.001 and ****P<0.0001, high vs. low. EMC3-AS1, endoplasmic reticulum membrane protein complex subunit 3 antisense RNA 1; mRNAsi, mRNA stemness index; EREG, epigenetically regulated; H-, high; L-, low.
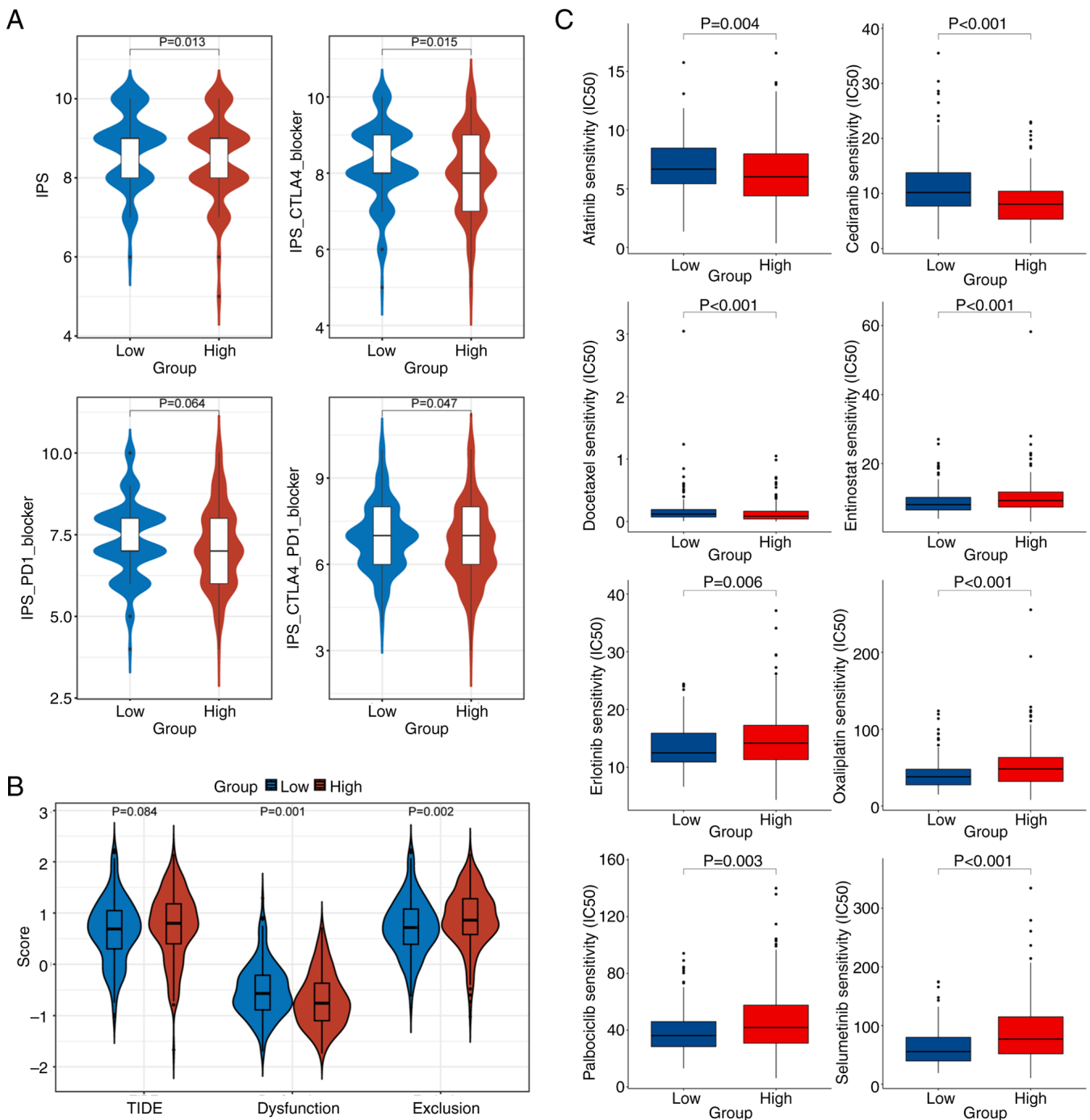
Figure 6. Value of *EMC3-AS1* for predicting the response to immunotherapy and systemic therapy in liver cancer. (A) Prediction of the ability of *EMC3-AS1* to block immune checkpoints according to *CTLA4* and *PD1* blocker status. (B) Comparison of tumor immune dysfunction and exclusion scores between H- and L-EMC3-AS1 expression groups. (C) Sensitivity analysis for eight anticancer drugs in H- and L-EMC3-AS1 expression groups. EMC3-AS1, endoplasmic reticulum membrane protein complex subunit 3 antisense RNA 1; CTLA4, cytotoxic T-lymphocyte antigen 4; PD1, programmed cell death protein 1; IPS, immunophenoscore; TIDE, tumor immune dysfunction and exclusion; IC50, half maximal inhibitory concentration; H, high; L, low.

the upregulation of PD ligand 1 (PD-L1) expression is a significant predictor of poor survival (46-48). Enhancing the response of a patient to anti-PD-1 or anti-PD-L1 treatment is a pivotal therapeutic strategy for patients with liver cancer (48). Notably, in the current study, the mRNA expression of several key ICIs, including *CTLA4*, *CD86*, *CD274*, *LGALS9*, *PDCD1* and *TIGIT*, was significantly higher in the H-EMC3-AS1 expression group than that in the L-EMC3-AS1 expression group. This finding suggests that patients exhibiting elevated

levels of *EMC3-AS1* also demonstrate increased expression of various ICs in the TME, which would be clinically helpful in improving patient stratification for IC blockade immunotherapy.

Clinical impact assessments of ICIs have been conducted in various cancer types, and drugs such as nivolumab, pembrolizumab and atezolizumab have been recommended as first-line treatments for patients with liver cancer (49). However, positive responses to immunotherapy are observed in only a
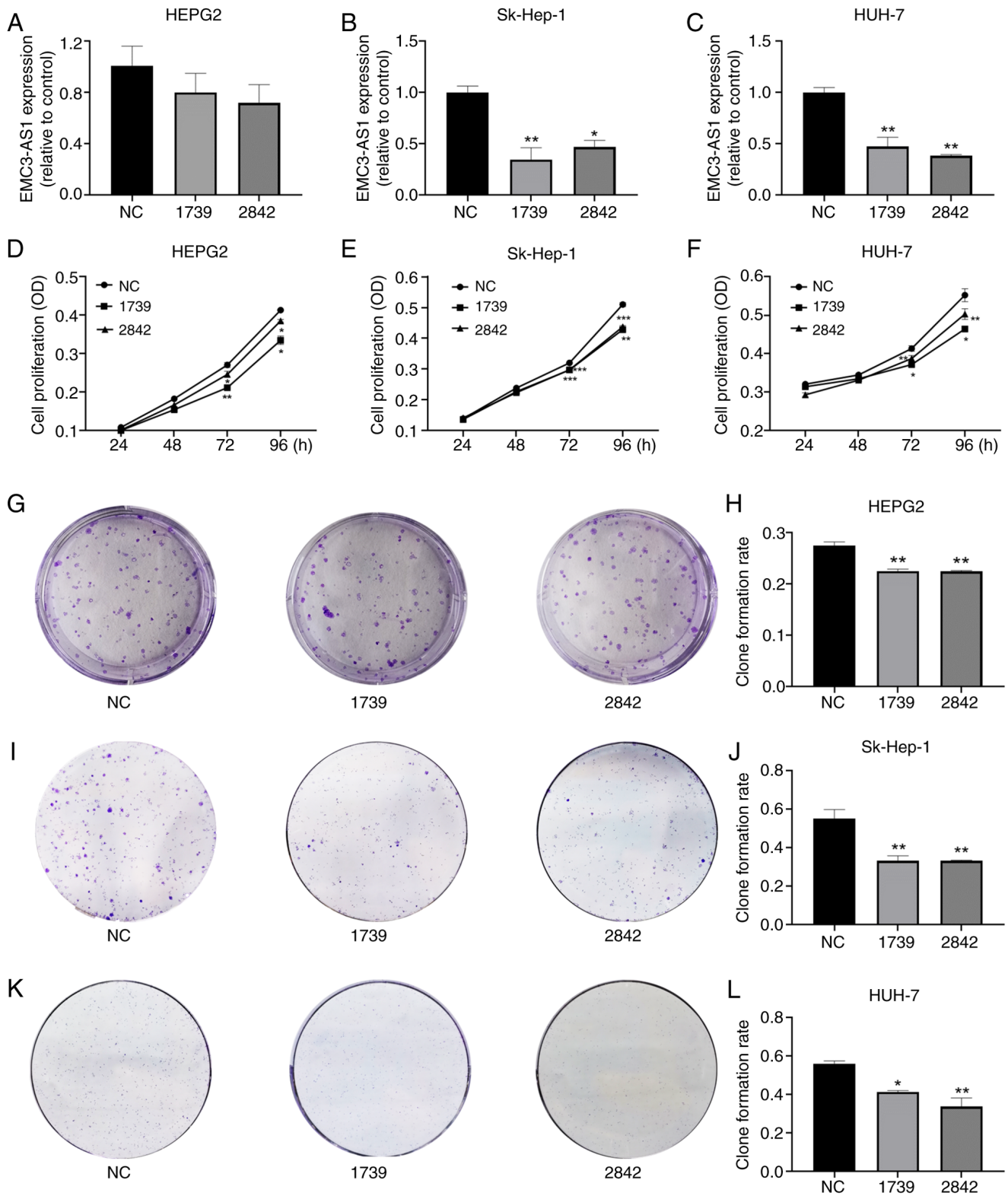
Figure 7. Effect of *EMC3-AS1* knockdown on the proliferation of liver cancer cells. The expression of *EMC3-AS1* was suppressed by transfection with siRNA-1739 and siRNA-2842 in (A) HepG2, (B) Sk-Hep-1 and (C) Huh-7 cells. The knockdown of *EMC3-AS1* expression inhibited the proliferation of (D) HepG2, (E) Sk-Hep-1 and (F) Huh-7 cells, as determined by MTT assay. (G-L) Colony forming assays revealed the inhibitory effect of knocking down *EMC3-AS1* expression on HepG2, Sk-Hep-1 and Huh-7 cells. Representative images of (G) HepG2, (I) Sk-Hep-1 and (K) Huh-7 colonies and colony formation rates for (H) HepG2, (J) Sk-Hep-1 and (L) Huh-7 are presented. $^*P<0.05$, $^{**}P<0.01$ and $^{***}P<0.001$ vs. the NC group. EMC3-AS1, endoplasmic reticulum membrane protein complex subunit 3 antisense RNA 1; siRNA, small interfering RNA; NC, negative control siRNA; OD, optical density.

small proportion of patients with liver cancer, highlighting the importance of identifying responsive patients and understanding resistance mechanisms (50). In the present study,

patients with liver cancer with low *EMC3-AS1* expression had higher IPSs when strategies to block CTLA4 or co-block PD1 and CTLA4 were employed. Additionally, patients with low
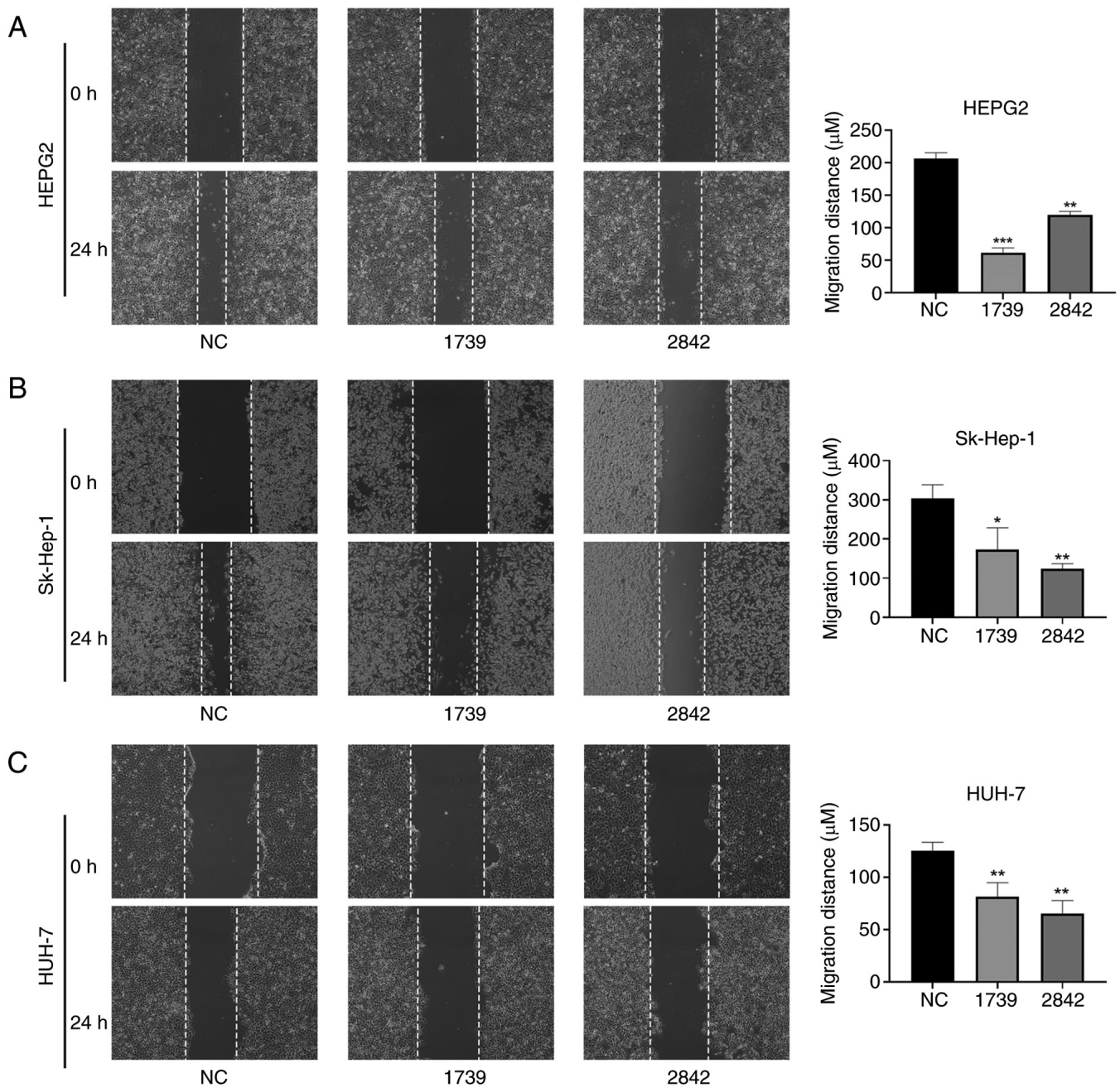
Figure 8. Effect of *EMC3-AS1* knockdown by transfection with siRNA-1739 and siRNA-2842 on the migration of liver cancer cells assessed via wound healing assay. The results showed that the migration ability of (A) HepG2, (B) Sk-Hep-1 and (C) Huh-7 cells was suppressed by the knockdown of *EMC3-AS1* expression. *P<0.05, **P<0.01 and ***P<0.001 vs. the NC group. EMC3-AS1, endoplasmic reticulum membrane protein complex subunit 3 antisense RNA 1; siRNA, small interfering RNA; NC, negative control siRNA.

EMC3-AS1 expression exhibited higher dysfunction scores and lower exclusion scores for T cells, indicating that they were more likely to benefit from immunotherapy.

Further experiments were performed in the present study to investigate the influence of *EMC3-AS1* on the biological behavior of liver cancer cells *in vitro*. Transfection with siRNA targeting *EMC3-AS1* markedly reduced its expression in HepG2, Sk-Hep-1 and Huh-7 cells, leading to decreased cell proliferation and colony-forming ability. In addition, the results of wound healing and Transwell assays revealed that the migration capabilities of HepG2, Sk-Hep-1 and Huh-7 cells were notably suppressed following the downregulation of

EMC3-AS1 expression. These findings imply that *EMC3-AS1* may act as a potential target for the treatment of liver cancer.

However, the current study has several limitations that should be acknowledged. Firstly, multicenter studies with larger sample sizes are required to confirm the expression of *EMC3-AS1* in liver cancer. Secondly, additional experiments are required to explore the potential *in vitro* and *in vivo* mechanisms of *EMC3-AS1* to support the present findings. Thirdly, the CIBERSORT algorithm relies on the fidelity of the reference profiles, which could deviate in cells involved in heterotypic interactions, phenotypic plasticity or disease-induced dysregulation. It is necessary to verify
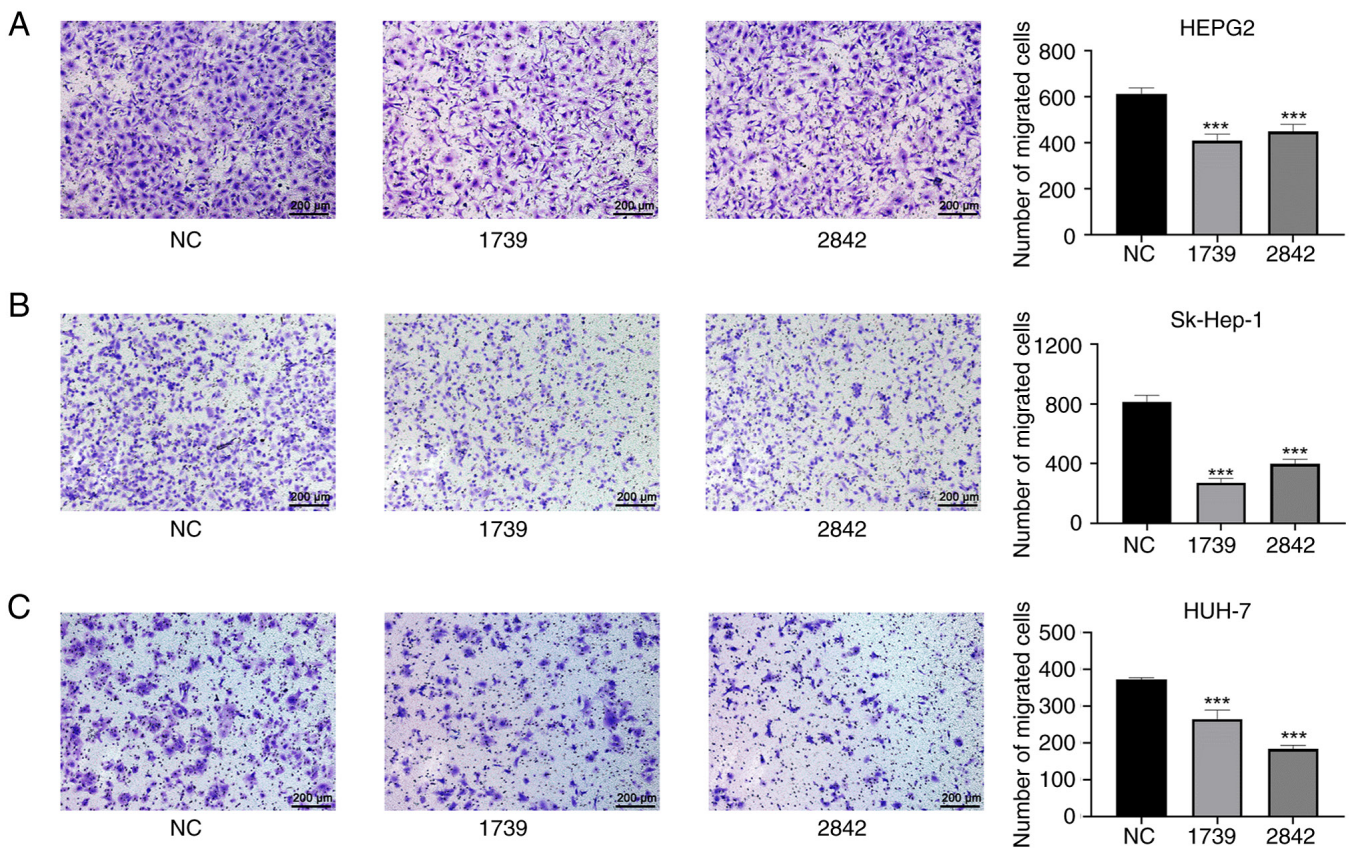
Figure 9. Effect of *EMC3-AS1* knockdown by transfection with siRNA-1739 and siRNA-2842 on the migration ability of liver cancer cells assessed using a Transwell assay. The results showed that the knockdown of *EMC3-AS1* expression in (A) HepG2, (B) Sk-Hep-1 and (C) Huh-7 cells inhibited the migration of the cells. ***$P<0.001$ vs. the NC group. EMC3-AS1, endoplasmic reticulum membrane protein complex subunit 3 antisense RNA 1; siRNA, small interfering RNA; NC, negative control siRNA.

results in independent cohorts or experimental models in future research. Finally, prospective studies are warranted to validate the prognostic and diagnostic value of *EMC3-AS1* in patients with liver cancer.

In summary, lncRNA *EMC3-AS1* is upregulated in liver cancer and is associated with a poor prognosis, making it a potential diagnostic and prognostic biomarker for patients with liver cancer. Silencing *EMC3-AS1* is potentially a promising therapeutic approach for liver cancer treatment.

Availability of data and materials

The data generated in the present study may be requested from the corresponding author.

Authors' contributions

BL designed the study and analyzed the data. XY performed the experiments. JZ and KD were involved in the acquisition and management of data. TF analysed the data and interpreted the results. BL, XY and TF revised the manuscript. CD designed the study and wrote the manuscript. BL and XY confirm the authenticity of all the raw data. All authors read and approved the final manuscript.

Ethics approval and consent to participate

This study was performed in accordance with the principles of the Declaration of Helsinki. Approval was granted by the Ethics Committee of Sichuan Provincial People's Hospital (Chengdu, China; approval no. 2022-2). Written informed consent for the use of their tissues was acquired from patients before surgery.

Patient consent for publication

Not applicable.

Competing interests

The authors declare that they have no competing interests.

References

1. Sung H, Ferlay J, Siegel RL, Laversanne M, Soerjomataram I, Jemal A and Bray F: Global cancer statistics 2020: GLOBOCAN estimates of incidence and mortality worldwide for 36 cancers in 185 countries. CA Cancer J Clin 71: 209-249, 2021.

2. Nagtegaal ID, Odze RD, Klimstra D, Paradis V, Rugge M, Schirmacher P, Washington KM, Carneiro F and Cree IA; WHO Classification of Tumours Editorial Board: The 2019 WHO classification of tumours of the digestive system. Histopathology 76: 182-188, 2020.

3. Zhang W, Hu B, Han J, Wang Z, Ma G, Ye H, Yuan J, Cao J, Zhang Z, Shi J, *et al*: Surgery after conversion therapy with PD-1 Inhibitors plus tyrosine kinase inhibitors are effective and safe for advanced hepatocellular carcinoma: A pilot study of ten patients. Front Oncol 11: 747950, 2021.

4. Caley DP, Pink RC, Trujillano D and Carter DRF: Long noncoding RNAs, chromatin, and development. ScientificWorldJournal 10: 90-102, 2010.

5. Jiang MC, Ni JJ, Cui WY, Wang BY and Zhuo W: Emerging roles of lncRNA in cancer and therapeutic opportunities. Am J Cancer Res 9: 1354-1366, 2019.

6. Huang Z, Zhou JK, Peng Y, He W and Huang C: The role of long noncoding RNAs in hepatocellular carcinoma. Mol Cancer 19: 77, 2020.

7. Liu Y, Liu X, Lin C, Jia X, Zhu H, Song J and Zhang Y: Noncoding RNAs regulate alternative splicing in cancer. J Exp Clin Cancer Res 40: 11, 2021.

8. Malakoti F, Targhazeh N, Karimzadeh H, Mohammadi E, Asadi M, Asemi Z and Alemi F: Multiple function of lncRNA MALAT1 in cancer occurrence and progression. Chem Biol Drug Des 101: 1113-1137, 2023.

9. Si C, Yang L and Cai X: LncRNA LINC00649 aggravates the progression of cervical cancer through sponging miR-216a-3p. J Obstet Gynaecol Res 48: 2853-2862, 2022.

10. Tang D, Zhao L, Peng C, Ran K, Mu R and Ao Y: LncRNA CRNDE promotes hepatocellular carcinoma progression by upregulating SIX1 through modulating miR-337-3p. J Cell Biochem 120: 16128-16142, 2019.

11. Cai Y, Lyu T, Li H, Liu C, Xie K, Xu L, Li W, Liu H, Zhu J, Lyu Y, *et al*: LncRNA CEBPA-DT promotes liver cancer metastasis through DDR2/β-catenin activation via interacting with hnRNPC. J Exp Clin Cancer Res 41: 335, 2022.

12. Zhao Z, Gao J and Huang S: LncRNA SNHG7 promotes the HCC progression through miR-122-5p/FOXK2 axis. Dig Dis Sci 67: 925-935, 2022.

13. Ji Y, Sun H, Liang H, Wang Y, Lu M, Guo Z, Lv Z and Ren W: Evaluation of LncRNA ANRIL potential in hepatic cancer progression. J Environ Pathol Toxicol Oncol 38: 119-131, 2019.

14. Dai D, Wang H, Zhu L, Jin H and Wang X: N6-methyladenosine links RNA metabolism to cancer progression. Cell Death Dis 9: 124, 2018.

15. Ma S, Chen C, Ji X, Liu J, Zhou Q, Wang G, Yuan W, Kan Q and Sun Z: The interplay between m6A RNA methylation and noncoding RNA in cancer. J Hematol Oncol 12: 121, 2019.

16. Burchard J, Zhang C, Liu AM, Poon RT, Lee NP, Wong KF, Sham PC, Lam BY, Ferguson MD, Tokiwa G, *et al*: microRNA-122 as a regulator of mitochondrial metabolic gene network in hepatocellular carcinoma. Mol Syst Biol 6: 402, 2010.

17. Sung WK, Zheng H, Li S, Chen R, Liu X, Li Y, Lee NP, Lee WH, Ariyaratne PN, Tennakoon C, *et al*: Genome-wide survey of recurrent HBV integration in hepatocellular carcinoma. Nat Genet 44: 765-769, 2012.

18. Makowska Z, Boldanova T, Adametz D, Quagliata L, Vogt JE, Dill MT, Matter MS, Roth V, Terracciano L and Heim MH: Gene expression analysis of biopsy samples reveals critical limitations of transcriptome-based molecular classifications of hepatocellular carcinoma. J Pathol Clin Res 2: 80-92, 2016.

19. Pugh RN, Murray-Lyon IM, Dawson JL, Pietroni MC and Williams R: Transection of the oesophagus for bleeding oesophageal varices. Br J Surg 60: 646-649, 1973.

20. Livak KJ and Schmittgen TD: Analysis of relative gene expression data using real-time quantitative PCR and the 2(-Delta Delta C(T)) method. Methods 25: 402-408, 2001.

21. Robin X, Turck N, Hainard A, Tiberti N, Lisacek F, Sanchez JC and Müller M: pROC: An open-source package for R and S+ to analyze and compare ROC curves. BMC Bioinformatics 12: 77, 2011.

22. Hänzelmann S, Castelo R and Guinney J: GSVA: Gene set variation analysis for microarray and RNA-seq data. BMC Bioinformatics 14: 7, 2013.

23. Subramanian A, Tamayo P, Mootha VK, Mukherjee S, Ebert BL, Gillette MA, Paulovich A, Pomeroy SL, Golub TR, Lander ES and Mesirov JP: Gene set enrichment analysis: A knowledge-based approach for interpreting genome-wide expression profiles. Proc Natl Acad Sci USA 102: 15545-15550, 2005.

24. Yu G, Wang LG, Han Y and He QY: clusterProfiler: An R package for comparing biological themes among gene clusters. OMICS 16: 284-287, 2012.

25. Ritchie ME, Phipson B, Wu D, Hu Y, Law CW, Shi W and Smyth GK: limma powers differential expression analyses for RNA-sequencing and microarray studies. Nucleic Acids Res 43: e47, 2015.

26. Edge SB and Compton CC: The American joint committee on cancer: The 7th edition of the AJCC cancer staging manual and the future of TNM. Ann Surg Oncol 17: 1471-1474, 2010.

27. Newman AM, Steen CB, Liu CL, Gentles AJ, Chaudhuri AA, Scherer F, Khodadoust MS, Esfahani MS, Luca BA, Steiner D, *et al*: Determining cell type abundance and expression from bulk tissues with digital cytometry. Nat Biotechnol 37: 773-782, 2019.

28. Salmaninejad A, Valilou SF, Shabgah AG, Aslani S, Alimardani M, Pasdar A and Sahebkar A: PD-1/PD-L1 pathway: Basic biology and role in cancer immunotherapy. J Cell Physiol 234: 16824-16837, 2019.

29. Malta TM, Sokolov A, Gentles AJ, Burzykowski T, Poisson L, Weinstein JN, Kamińska B, Huelsken J, Omberg L, Gevaert O, *et al*: Machine learning identifies stemness features associated with oncogenic dedifferentiation. Cell 173: 338-354.e15, 2018.

30. Yoshihara K, Shahmoradgoli M, Martínez E, Vegesna R, Kim H, Torres-Garcia W, Treviño V, Shen H, Laird PW, Levine DA, *et al*: Inferring tumour purity and stromal and immune cell admixture from expression data. Nat Commun 4: 2612, 2013.

31. Charoentong P, Finotello F, Angelova M, Mayer C, Efremova M, Rieder D, Hackl H and Trajanoski Z: Pan-cancer immunogenomic analyses reveal genotype-immunophenotype relationships and predictors of response to checkpoint blockade. Cell Rep 18: 248-262, 2017.

32. Jiang P, Gu S, Pan D, Fu J, Sahu A, Hu X, Li Z, Traugh N, Bu X, Li B, *et al*: Signatures of T cell dysfunction and exclusion predict cancer immunotherapy response. Nat Med 24: 1550-1558, 2018.

33. Maeser D, Gruener RF and Huang RS: oncoPredict: An R package for predicting in vivo or cancer patient drug response and biomarkers from cell line screening data. Brief Bioinform 22: bbab260, 2021.

34. Chew V, Lai L, Pan L, Lim CJ, Li J, Ong R, Chua C, Leong JY, Lim KH, Toh HC, *et al*: Delineation of an immunosuppressive gradient in hepatocellular carcinoma using high-dimensional proteomic and transcriptomic analyses. Proc Natl Acad Sci USA 114: E5900-E5909, 2017.

35. Dunn GP, Bruce AT, Ikeda H, Old LJ and Schreiber RD: Cancer immunoediting: From immunosurveillance to tumor escape. Nat Immunol 3: 991-998, 2002.

36. Shlomai A, de Jong YP and Rice CM: Virus associated malignancies: The role of viral hepatitis in hepatocellular carcinoma. Semin Cancer Biol 26: 78-88, 2014.

37. Pardoll DM: The blockade of immune checkpoints in cancer immunotherapy. Nat Rev Cancer 12: 252-264, 2012.

38. Margetts J, Ogle LF, Chan SL, Chan AWH, Chan KCA, Jamieson D, Willoughby CE, Mann DA, Wilson CL, Manas DM, *et al*: Neutrophils: Driving progression and poor prognosis in hepatocellular carcinoma? Br J Cancer 118: 248-257, 2018.

39. Arvanitakis K, Mitroulis I and Germanidis G: Tumor-associated neutrophils in hepatocellular carcinoma pathogenesis, prognosis, and therapy. Cancers (Basel) 13: 2899, 2021.

40. Wang HC, Haung LY, Wang CJ, Chao YJ, Hou YC, Yen CJ and Shan YS: Tumor-associated macrophages promote resistance of hepatocellular carcinoma cells against sorafenib by activating CXCR2 signaling. J Biomed Sci 29: 99, 2022.

41. You M, Gao Y, Fu J, Xie R, Zhu Z, Hong Z, Meng L, Du S, Liu J, Wang FS, *et al*: Epigenetic regulation of HBV-specific tumor-infiltrating T cells in HBV-related HCC. Hepatology 78: 943-958, 2023.

42. Zhu AX, Finn RS, Edeline J, Cattan S, Ogasawara S, Palmer D, Verslype C, Zagonel V, Fartoux L, Vogel A, *et al*: Pembrolizumab in patients with advanced hepatocellular carcinoma previously treated with sorafenib (KEYNOTE-224): A non-randomised, open-label phase 2 trial. Lancet Oncol 19: 940-952, 2018.

43. Romano E, Kusio-Kobialka M, Foukas PG, Baumgaertner P, Meyer C, Ballabeni P, Michielin O, Weide B, Romero P and Speiser DE: Ipilimumab-dependent cell-mediated cytotoxicity of regulatory T cells ex vivo by nonclassical monocytes in melanoma patients. Proc Natl Acad Sci USA 112: 6140-6145, 2015.

44. Powles T, Eder JP, Fine GD, Braiteh FS, Loriot Y, Cruz C, Bellmunt J, Burris HA, Petrylak DP, Teng SL, *et al*: MPDL3280A (anti-PD-L1) treatment leads to clinical activity in metastatic bladder cancer. Nature 515: 558-562, 2014.

45. Rotte A, Jin JY and Lemaire V: Mechanistic overview of immune checkpoints to support the rational design of their combinations in cancer immunotherapy. Ann Oncol 29: 71-83, 2018.

46. Shi J, Liu J, Tu X, Li B, Tong Z, Wang T, Zheng Y, Shi H, Zeng X, Chen W, *et al*: Single-cell immune signature for detecting early-stage HCC and early assessing anti-PD-1 immunotherapy efficacy. J Immunother Cancer 10: e003133, 2022.

47. Pfister D, Núñez NG, Pinyol R, Govaere O, Pinter M, Szydlowska M, Gupta R, Qiu M, Deczkowska A, Weiner A, *et al*: NASH limits anti-tumour surveillance in immunotherapy-treated HCC. Nature 592: 450-456, 2021.

48. Cheng AL, Hsu C, Chan SL, Choo SP and Kudo M: Challenges of combination therapy with immune checkpoint inhibitors for hepatocellular carcinoma. J Hepatol 72: 307-319, 2020.

49. Benson AB, D'Angelica MI, Abbott DE, Anaya DA, Anders R, Are C, Bachini M, Borad M, Brown D, Burgoyne A, *et al*: Hepatobiliary cancers, version 2.2021, NCCN clinical practice guidelines in oncology. J Natl Compr Canc Netw 19: 541-565, 2021.

50. Federico P, Petrillo A, Giordano P, Bosso D, Fabbrocini A, Ottaviano M, Rosanova M, Silvestri A, Tufo A, Cozzolino A and Daniele B: Immune checkpoint inhibitors in hepatocellular carcinoma: Current status and novel perspectives. Cancers (Basel) 12: 3025, 2020.